ELSEVIER

Ceramics International 25 (1999) 207–213

CERAMICS INTERNATIONAL

Effect of different rare earth cations on the densification behaviour of oxygen rich α-SiAlON composition

S. Bandyopadhyay [a,*], M.J. Hoffmann [b], G. Petzow [c]

[a] *Central Glass & Ceramic Research Institute, Calcutta 700 032, India*
[b] *Institute for Ceramics in Mechanical Engineering, University of Karlsruhe, Haid- und Neu Str. 7, D 76131, Karlsruhe, Germany*
[c] *Max Plack Institute, Powder Metallurgical Laboratory, Heisenbergstr. 5, D 70569, Stuttgart, Germany*

Received 25 September 1997; accepted 27 February 1998

Abstract

Five different stabilizing cations (Y, Yb, Dy, Sm, Nd) were investigated on an α-SiAlON composition, deliberately shifted to the Al_2O_3 rich area corresponding to $M_{0.445}Si_{9.998}Al_{2.003}O_{0.668}N1_{5.333,}$ with respect to the reaction sequences, densification behaviour and mechanical properties. The analysis of the reaction sequences show that the formation of α-SiAlON involves the intermediate formation of aluminate, garnet, melilite and a nitrogen rich liquid containing the respective cation. The sintering rate is influenced by volume fraction of the garnet and melilite phase which varies for different cations. Dy_2O_3 shows the best densification behaviour which is followed by Sm_2O_3 and Nd_2O_3. The fracture toughness for all are comparable while the hardness value seems to decrease with the increasing ionic size of the cations due to the lower proportions of α-SiAlON phase. The present composition favours the removal of melilite from the as cooled product as well as good densification.

1. Introduction

SiAlON ceramics are promising candidates for engineering applications because of the combination of some excellent intrinsic mechanical, thermal and chemical properties [1,2]. α-SiAlON (α′) exists in the M-Si-Al-O-N system [3–8] where M stands for metal like Li, Ca, Mg, Y and some of the rare earth metals except Ce, La, Pr and Eu [7,8]. It is based on the (α-Si_3N_4 structure where a part of Si^{4+} is substituted by Al^{3+} and the valency compensation is made partly by the incorporation of O^{2-} in the sites of N^{3-} and the rest by the stuffing of M cations into the interstitial holes. The material has a general formula of $M_mSi_{12-(pm+n)}Al_{pm+n}O_nN_{16-n}$ for a metal ion with valency p+.

Extensive phase relation and properties studies have been made earlier in the yttrium containing system [3–18]. α-SiAlON is extended in a narrow two dimensional compositional field in the plane Si_3N_4–Al_2O_3.AlN–YN.3AlN of the system Si_3N_4–AlN–YN–SiO_2–Al_2O_3–Y_2O_3. Recent studies [7,19–30] are focused on the formation of α-SiAlON stabilized with rare earth metals, viz., Ytterbium, Dysprosium, Samarium, Neodymium, etc. The compositional field for stabilization of α-SiAlON with different rare earth metals are quite similar but widens slightly with decreasing size of the cations [7,8]. These rare earth oxides are reported [24,28] to promote more fluid transient liquid during sintering than yttria and hence an easier densification is expected. Dy_2O_3 has been reported to be the most effective one [28].

The sintering of α′ is difficult when some secondary and intermediate phases appear in the product. These phases consume a major portion of the sintering additive and become competitive for α′ formation and also to the densification process. For example, densification more than 96% of theoretical under pressureless sintering could not be achieved [28] in the case of four rare earth cations ytterbium, dysprosium, samarium and neodymium replacing yttrium due to the presence of nitrogen melilite ($M_2Si_{3-x}Al_xO_{3+x}N_{4-x}$, where M stands for Dy, Sm, Yb, Y, [31,32] etc.) The sensitivity of the α′ formation to these phases has been studied earlier in Y-Si-Al-O-N system [15,17,18,33,34]. However, the detailed knowledge of the course of reaction with the other rare earth additive systems is not available.

* Corresponding author.

0272-8842/99/$—see front matter
PII: S0272-8842(98)00025-X

In general, HIPing [14,21] or hot pressing [23,28–30] is required particularly when the α′ composition is taken on the stoichiometric line joining Si_3N_4-M_2O_3.9AlN. The majority of the available properties are therefore reported from the hot pressed materials. Recently, an improved densification under pressureless sintering condition is observed in the case of yttrium-α′ when the composition is shifted slightly from the stoichiometric line towards Al_2O_3 rich side of the plane Si_3N_4-Y_2O_3.9AlN-Al_2O_3.AlN [18]. In the present study, this new composition is considered with four rare earth cations ytterbium, dysprosium, samarium and neodymium replacing yttrium and the reaction sequences of the formation of α′ is studied. The densification behaviour and a few mechanical properties for the materials densified under pressureless sintering conditions are also studied and is discussed with reference to the available data on stoichiometric α′ composition.

2. Experimental procedure

The basic composition is located along a line parallel to the join Si_3N_4–M_2O_3.9AlN but is shifted to the Al_2O_3 rich side which intersects the join Si_3N_4–Al_2O_3.AlN at 2.53 eq% Oxygen corresponding to a z-value of β-SiAlON (β′) of 0.15 in the general formula $Si_{3-z}Al_zO_zN_{4-z}$. The composition corresponds to $M_{0.445}Si_{9.998}Al_{2.003}O_{0.668}N_{15.333}$ and falls within the two dimensional stability zone of α′ along the plane Si_3N_4–Y_2O_3.9AlN-Al_2O_3.AlN in the system Y–Si–Al–O–N [6]. The starting powders Si_3N_4 (UBE E10, UBE Industries, Japan), Al_2O_3 (Aluminalux 49 SG, Alcoa, USA), AlN (grade 3, H.C. Starck, Germany), Y_2O_3, Yb_2O_3, Dy_2O_3, Sm_2O_3, and Nd_2O_3 (fine grade, H.C. Starck, Germany) were attrition milled with Si_3N_4 milling balls using isopropanol as milling media. The powder mixtures were subsequently dried, sieved and consolidated into cylinders with a diameter of 15 mm and a height of 12 mm by using rubber moulds and cold isostatic pressing at a pressure of 630 MPa. The samples were fired in a BN crucible in a graphite resistance heating furnace (Thermal Technology, USA) under 1 MPa nitrogen pressure as well as in a high temperature dilatometer under 0.1 MPa nitrogen. To analyze the formation of transient phases during sintering, specimens were quenched from a given temperature to room temperature with a cooling rate of approximately 60°C/min. The final density was measured by Archimedes method in distilled water and the phases were identified by XRD using Cu Kα radiation. Samples for microstructural observation were ground and polished with 1 μm diamond paste. The hardness and fracture toughness were determined with a Vickers diamond indentor using 10 kg load [35].

3. Results & discussion

3.1. Reaction sequences

The dilatometric study was performed for all samples with a linear heating rate of 15°C/min under nitrogen gas at ambient pressure (Fig. 1). The derived shrinkage rate (Fig. 2), when studied in association with the phases present, reveals the reaction sequences of formation of α′ in the final product. For all the compositions, shrinkage starts from 1250-1300°C. In case of yttrium-SiAlON, this coincides with the formation of YAM ($Y_4Al_2O_9$). The total shrinkage at this temperature is small. With further rise in temperature the sintering rate curve shows three maxima. The first one at around 1350°C is attributed to the formation of an oxide melt in the system Y_2O_3–Al_2O_3–SiO_2, the SiO_2 being the oxide impurity of the Si_3N_4 powder [33]. This part also has a negligible contribution to the overall shrinkage. Above 1400°C, YAG ($Y_3Al_5O_{12}$) crystallizes out of the liquid and causes a reduction in the shrinkage rate. When the temperature exceeds 1500°C, a larger amount of the liquid phase appears with the simultaneous dissolution of YAG into it. AlN and α-Si_3N_4 also start to dissolve in the liquid thereby turning it to be an oxynitride one from which α′ starts precipitating. This brings a larger extent of sintering and forms the second maxima in the rate curve. Above 1600°C, the sintering rate falls down for a second time due to the precipitation of another crystalline phase, melilite, from the oxynitride melt. As a considerable portion of the cations are consumed by melilite, the volume fraction of liquid is reduced and hence the fall in the sintering rate. With further rise in temperature, this phase is redissolved like the previous one (garnet) resulting in a larger amount of liquid to reappear. This contributes to the majority of densification and produces the third maxima. The reaction sequences are similar to that of the α′ compositions taken along the stoichiometric line joining Si_3N_4–Y_2O_3.9AlN [34].

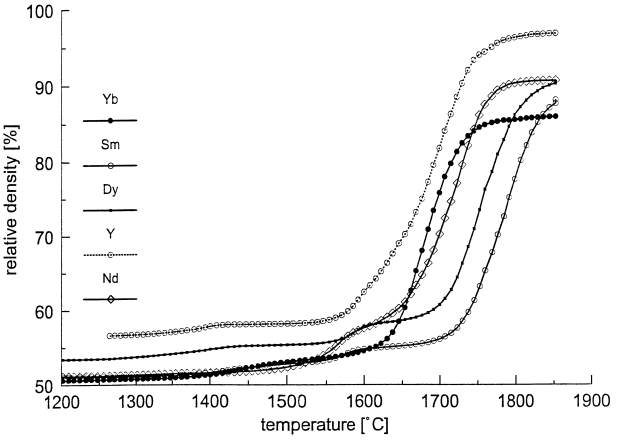

Fig. 1. Change of the density of the investigated compositions as a function of temperature.

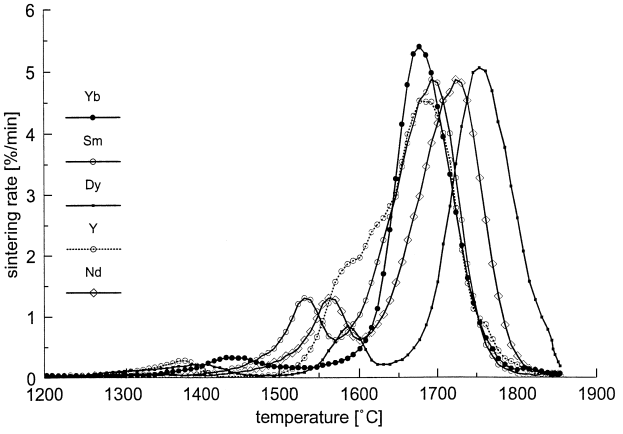

Fig. 2. Derived sintering rate of the investigated compositions as a function of temperature.

The Dy-, Sm- and Nd- containing samples follow the exactly similar behaviour of the Y- containing composition. The only difference lies in the amount of melilite formation, the temperature at which this phase appears and the temperature range over which the stability of this phase is extended. For both Sm and Nd, the precipitation of melilite commences earlier in comparison to Dy. The amount of this phase as appeared from XRD, is highest in case of Nd, closely followed by Sm, much lesser in Dy and is minimum in case of Y. The stability of Dy-melilite is very similar to Y-melilite which disappears within a very narrow temperature range. On the other hand, for both Sm and Nd, only a part of this phase goes into solution while a considerable amount remains up to a high sintering temperature of 1750°C for Sm and 1800°C for Nd- containing samples. However, the Yb- added sample shows only the first two maxima in the sintering rate curve. The garnet phase, in this case, is much extended with rising temperature whereas melilite is completely absent.

3.2. Appearances of phases

The ultimate phases after 2 h of sintering under 1 MPa for all compositions are summarized in Table 1. The Y- stabilized sample shows α' as only crystalline phase in the entire temperature range. A similar material is obtained from both Yb- and Dy- added samples at >1750°C and Sm- added sample at >1800°C. The present Nd- containing composition differs from rest of the family and produced always a mixture of α' and β' (Fig. 3). The increasing amount of α' with temperature may be attributed to the availability of the stabilizing cation which comes from the simultaneous dissolution of a third phase, melilite, into the liquid [34]. For all samples in the lower temperature region, although the α' phase is still the major one, it is associated with some secondary phases those appeared in the intermediate stages of sintering and remain in the final product after

Table 1
Crystalline phases of the different compositions after 2 h sintering under 1 MPa nitrogen; α'- α-sialon, β'- β-sialon, M- nitrogen melilite ($Ln_2Si_{3-x}Al_xO_{3+x}N_{4-x}$, Ln = Nd, Sm, and Dy), G- ytterbium-aluminogarnet ($Yb_3Al_5O_{12}$)

Temperature (°C)	Stabilizing cations				
	Nd	Sm	Dy	Yb	Y
1900	$\alpha' > \beta'$	α'	α'	α'	α'
1850	$\alpha' > \beta'$	α'	α'		
1800	$\alpha' > \beta' > > M$	α'	α'	α'	α'
1750	$\alpha' > M > \beta'$	$\alpha' > > M$	α'	α'	α'
1650	$M > \alpha' > \beta'$	$\alpha' > M > > \beta'$	$\alpha' > > M$	$\alpha' > G$	α'

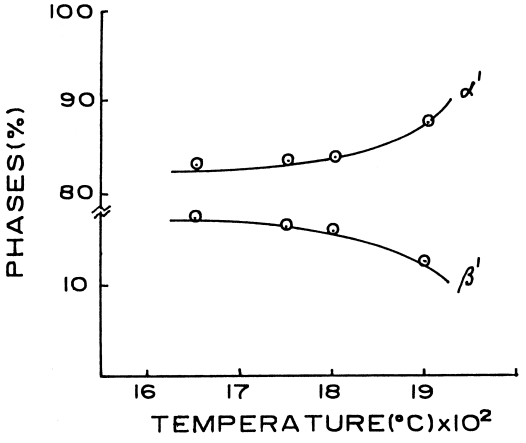

Fig. 3. Changes of the volume fraction of α' and β' as a function of temperature after 2 h isothermal sintering under 1 MPa nitrogen for Nd- added composition.

2 h of firing under isothermal treatment. Ytterbium garnet ($Yb_3Al_5O_{12}$) is the minor remnant phase for Yb while that for the others is melilite. The amount of melilite increases in the order of ionic size of the stabilizing cations as follows : Nd > Sm > Dy. This is consistent with the previous observations [22,26,28] where the involvement of larger amount of melilite in case of Nd- α' composition is reported in comparison to that containing Sm.

The appearances of phases in the present composition are similar to the α'-compositions taken on the stoichiometric line joining Si_3N_4 and M_2O_3.9AlN compound for both Sm [29] and Nd [30]. The only difference in this case is that the melilite phase did not appear even when the product was cooled with a slow cooling rate of $\sim$ 60°C/min in place of quenching ($\sim$ 400°C/min) as required earlier [29,30]. The similar advantage of this slightly Al_2O_3 rich composition for removal of the third phase from a composite containing α' and SiAlON polytype phases is already seen in case of Y–Si–Al–O–N system [18].

The present phase ratio, $\alpha'/\alpha' + \beta'$, for all the compositions may be compared to that of the previous work

(Fig. 4). It may be noted that the starting compositions are different in each case. For Ekstrom et al [21], it coincided with the region containing α' and β' whereas that for Wang et al [23] to the stoichiometric α' composition with $m=0.36$ (the α' may be represented as $M_mSi_{12-4.5m}Al_{4.5m}O_{1.5m}N_{16-1.5m}$ for a metal cation M with a valency of 3). The later studies also show that α' with m- value <0.4 always produce a mixture of $\alpha'+\beta'$ phases irrespective of the stabilizing cations, viz., Y [14], Sm [29], Nd [30]. For the present study, it is equivalent to $m=0.45$ and the nature of the crystalline phases with respect to the stabilizing cations is consistent to those of the previous findings [14,29,30]. One important point to note is that this paper only reports the formation behaviour of α' after sintering for 2 h. The phase ratio will, however, decrease due to the unstability of α' phase at $<1650°C$ when a post sintering heat treatment is undertaken [36–40]. The final ratio is controlled by the heat treatment temperature and time and offers an excellent mechanism in obtaining optimized microstructure in case of α'-β' [36].

3.3. Densification behaviour

The final densities and weight losses for all the samples fired at 1650 to 1900°C under 1 MPa nitrogen for 2 h are summarized in Table 2. Both Nd and Sm samples present a closely similar behaviour. At 1650°C, the density values reach only up to 85% TD. Since a portion of the stabilizing cations form melilite, and furthermore the Sm- and Nd- containing melilite has higher melting points [22,24,28–30], the poorer sinterability is attributed to the low amount of liquid phase. At higher firing temperature, the densities are >98% TD. The porosity has been estimated by a quantitative microstructural analysis under optical microscopy (Table 3) and SEM. In majority of the samples, the observed porosities corroborate these estimated from the theoretical density values. The Y- containing sample shows a poorer sinterability in comparison to that of Sm and Nd. The Yb sample shows the worst densification behaviour. The sample contains large pores distributed throughout (Fig. 5). The poorer sintering behaviour of both Yb- and Y- containing compositions in comparison to the other three cations is expected due to the following reasons : (i) the former two cations produce at sintering temperature liquids with higher viscosity [24]; (ii) the eutectic temperatures in the systems containing the former two cations are higher [28].

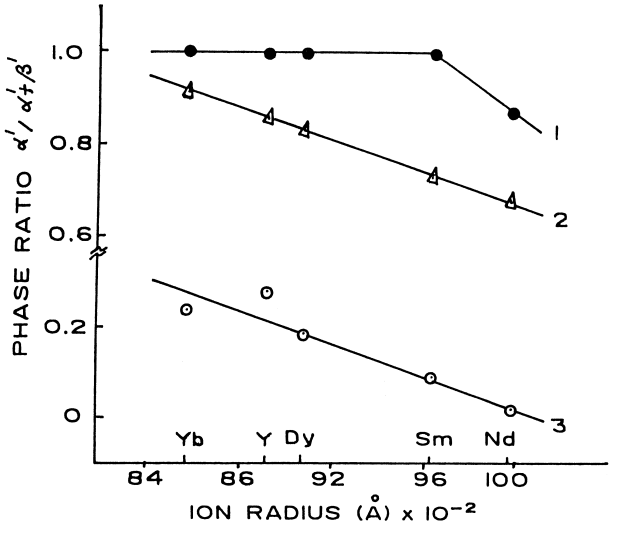

Fig. 4. Change of the $\alpha'/\alpha'+\beta'$ ratio as a function of the stabilizing cations; 1- present work, 2- reference 23, 3- reference 21.

Table 2
Densities and weight losses of different compositions after 2 h sintering under 1 MPa nitrogen

Stabilizing cations	Density ($g.cm^{-3}$)						Weight loss (%)
	1650°C	1750°C	1800°C	1825°C	1850°C	1900°C	
Nd	2.989	3.388	3.408	3.414	3.412	3.414	2.15-2.71
Sm	2.992	3.401	3.426	3.43	3.422	3.429	1.58-2.30
Dy	3.446	3.446	3.47	3.472	3.477	3.48	0.99-1.35
Yb	3.202	3.291	3.394	3.387	3.406	3.218	1.09-1.48
Y	3.284	3.289	3.299	3.297	3.32	3.301	0.96-1.14

Table 3
Percentage porosities of the sintered compositions at 1900°C for 2 h under 1 MPa nitrogen as estimated by different methods; porosities were counted by point counting method and is an average value of data from five photographs for each sample

Method of measurement	Stabilizing cations				
	Nd	Sm	Dy	Yb	Y
Microscopy	<0.5	<0.5	<0.5	9.6	6.4
Difference from TD	1.16	1.8	0.46	9.2	0.6

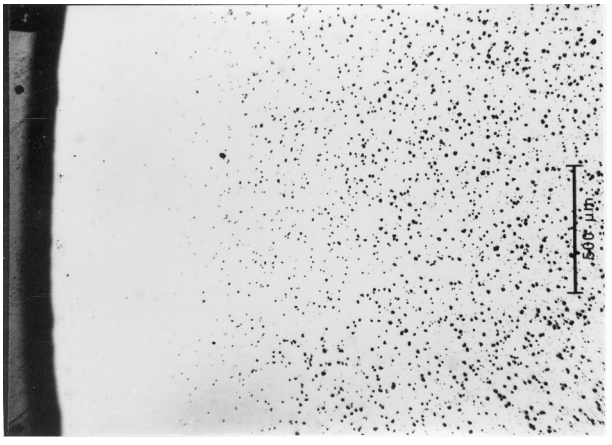

Fig. 5. Typical feature of the Yb added sample with a thin circumferencial dense layer followed by an increasing amount of porosity towards the core of the sample.

On the other hand, Dy- sample is the best one amongst all the compositions under study. On sintering above 1750°C, it shows >99% TD. The absence of any secondary crystalline phase and lower eutectic temperature in this system is responsible for such behaviour [28]. Hence, the sequence of stabilizing cations for better densification of the α′-composition under study may be described as follows : Dy > Sm, Nd > Y > Yb. It is also evident that a slight higher initial Al_2O_3 content in the starting composition provides good densification under pressureless sintering.

Table 4
Hardness and fracture toughness as a function of the stabilizing cations for samples sintered at 1850°C for 2 h under 1 MPa nitrogen; Each datum represents the average value of 20 measurements; bracketed values are standard deviations

Properties	Stabilizing cations				
	Nd	Sm	Dy	Yb	Y
K_{IC}	4.80	4.49	4.49	4.32	4.66
($MPa.m^{1/2}$)	(0.05)	(0.08)	(0.24)	(0.02)	(0.17)
Hardness	18.4	18.7	19.3	19.9	20.2
(GPa)	(0.4)	(0.4)	(0.5)	(0.4)	(0.4)

3.4. Properties

The Vickers hardness (HV_{10}) and the indentation fracture toughness (K_{IC}) for all the samples are presented in Table 4. The K_{IC} values are ranging in between 4.3 and 4.8 $MPa.m^{1/2}$ for different samples. It is evident that this property is not influenced by the size of the stabilizing cations for α′. A slight higher K_{IC} value for Nd- composition may be attributed to the reinforcement of the elongated in-situ grown β′ in the equiaxed α′ matrix [11,18,41] (Fig. 6). On the other hand, α′ is a very hard material with the highest hardness value corresponding to around 20 GPa obtained in cases of Yb- and Y- stabilized samples. This property seems to be dependent on the size of the stabilizing cations and decreases with the increasing ionic size. This is logical because for a specific composition, the amount of intergranular phase (which is softer) increases on moving to lower z- rare earth stabilizing cations [36] although the XRD establishes α′ as the only crystalline phase in the product. However, the presence of softer β′ phase is additionally responsible for lower hardness values of Nd- added sample.

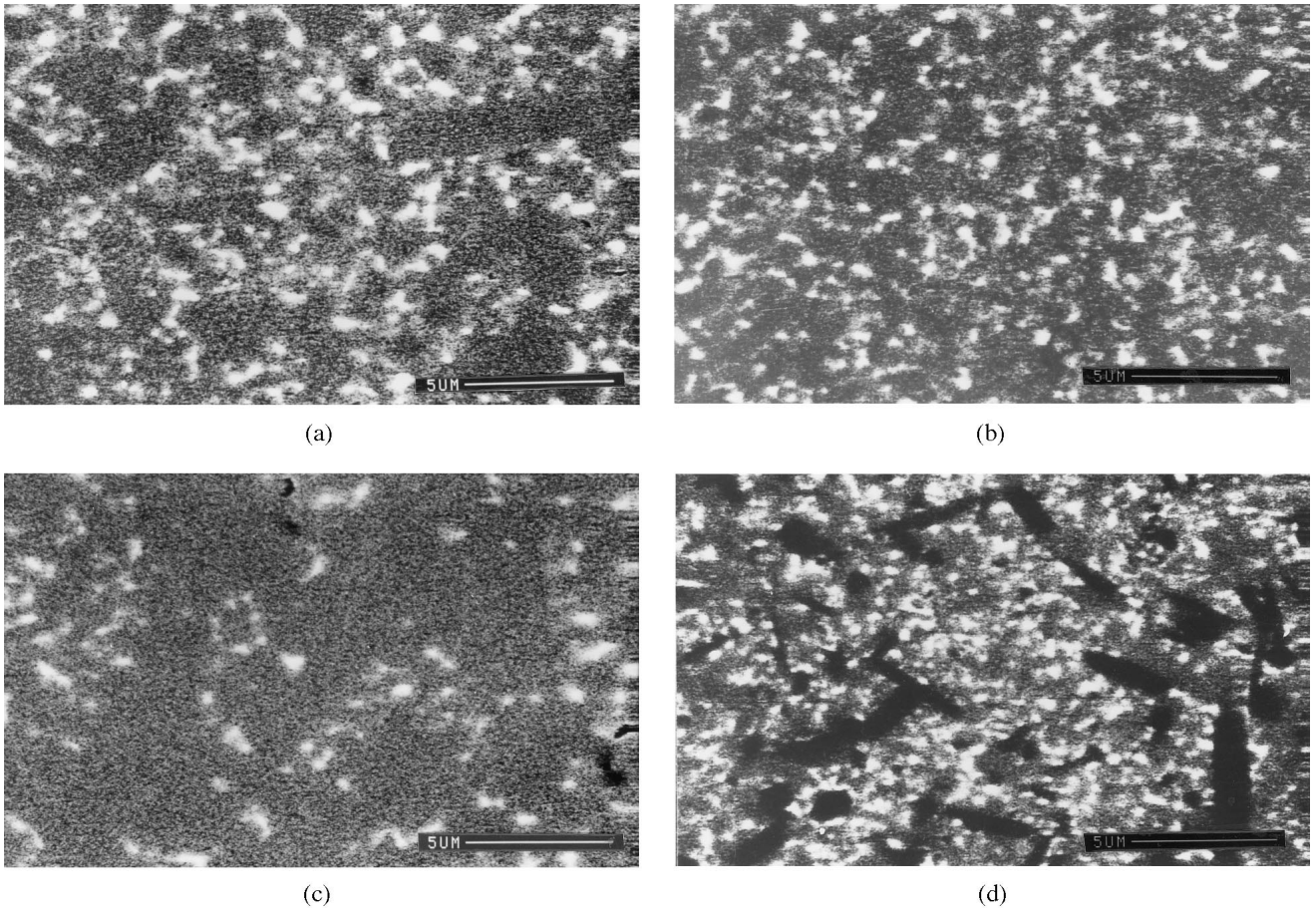

(a) (b) (c) (d)

Fig. 6. SEM micrographs of plasma etched (using a gas mixture of CF_4 and oxygen) surface of Nd- added composition; the darker and deeper etched particles are β′ grains whereas α′ grains reveal minor etching attack; bar -5 μm.

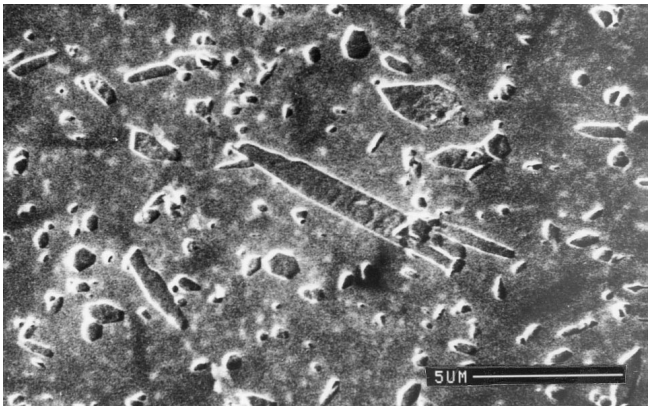

Fig. 7. SEM micrographs of plasma etched (using a gas mixture of CF_4 and oxygen) surface of Nd- added composition; the darker and deeper etched particles are β′ grains whereas α′ grains reveal minor etching attack; bar -5 μm.

4. Conclusions

α′ as single crystalline phase was obtained above 1650°C for Y-, above 1750°C for both Yb- and Dy- and above 1800°C for Sm- added sample in the present investigated composition. Nd produced always a mixture of α′ and β′ phases. The reaction sequences of formation of α′ involve the transient appearances of aluminate, garnet, melilite and a nitrogen rich liquid containing the respective additive cation. The sintering rate is controlled by volume fraction of the melilite phase formed which is maximum for Nd and is in the decreasing order for the others as follows : Sm > Dy > Y. On the other hand, Yb does not involve melilite but is similarly controlled by the presence of the garnet phase. Dy- added sample exhibits the best sinterability due to which the sintered density reaches above 99% TD above 1750°C. The overall densification behaviour for the different cations may be arranged as follows: Dy > Sm, Nd > Y > Yb. The fracture toughness for majority of the samples is similar while the hardness value seems to decrease with increasing ionic size of the stabilizing cations due to the decrease in α′ content. The results indicate that a small shift of the composition from the Si_3N_4-M_2O_3.9AlN union toward the Al_2O_3 rich side offers the advantages of the removal of melilite phase from the as cooled specimen and the commencement of good densification under pressureless sintering.

Acknowledgements

The work was carried out at Max Planck Institute, Stuttgart, Germany under DAAD-CSIR bilateral scientist exchange programme.

References

[1] K.H. Jack, Review: Sialons and related nitrogen ceramics, J. Mater. Sc. 11 (6) (1976) 1135–1158.
[2] T. Ekstrom, M. Nygren, Sialon ceramics, J. Am. Ceram. Soc. 75 (2) (1992) 259–276.
[3] S. Hampshire, H.K. Park, D.P. Thompson, K.H. Jack, α′ sialon ceramics, Nature (London) 274 (1978) 880–883.
[4] G. Grand, J. Demit, J. Ruste, J.P. Torr, Composition and stability of Y-Si-Al-O-N solid solutions based on α-Si_3N_4 structure, J. Mater. Sc. Lett. 14 (7) (1979) 1749–1751.
[5] Z.K. Huang, P. Greil, G. Petzow, Formation of α-Si_3N4 solid solutions in the system Si_3N_4-AlN-Al_2O_3, J. Am. Ceram. Soc. 66 (6) (1983) C96–97.
[6] D. Stutz, P. Greil, G. Petzow, Two dimensional solid solution formation of Y-containing α-Si_3N_4, J. Mater. Sc. Lett. 5 (3) (1986) 335–336.
[7] Z.K. Huang, T.Y. Tien, T.S. Yen, Subsolidous phase relationships in Si_3N_4-AlN-rare earth oxide systems, J. Am. Ceram. Soc. 69 (10) (1986) C241–242.
[8] W.Y. Sun, T.Y. Tien, T.-S. Yen, Solubility limits of α′-solid solutions in the system Si, Al, Y/N, O, J. Am. Ceram. Soc. 74 (1991) 2547–2550.
[9] S. Slasor, D.P. Thompson, Preparation and characterization of yttrium α-sialons, in: S. Hampshire (Ed.), Non Oxide Technical & Engineering Ceramics, Elsevier, Amsterdam, Netherlands, 1985, pp. 223–229.
[10] K. Ishizawa, N. Ayuzawa, A. Shiranita, M. Taki, N. Ushida, M. Mitomo, Properties of α-sialon ceramics, Yogyo Kyokaishi 94 (1986) 183–185.
[11] T. Ekstrom, Effect of composition, phase content and microstructure on the performance of yttrium sialon ceramics, Mater. Sc. Engg. A105/106 (1989) 341–349.
[12] G.Z. Cao, R. Metselaar, α′-sialon ceramics : A review, Chem. Mater. 3 (1991) 242–252.
[13] G.Z. Cao, R. Metselaar, G. Ziegler, Formation densification of α-sialon ceramics, in: P. Vincenzini (Ed.), Ceramics Today-Tomorrow's Ceramics, Elsevier Science Publishers B.V., Amsterdam, Netherlands, 1991, pp. 1285–1293.
[14] A. Bartek, T. Ekstrom, H. Herbertsson, T. Johansson, Yttrium α-sialon ceramics by hot pressing and post hot isostatic pressing, J. Am. Ceram. Soc. 75 (2) (1992) 432–439.
[15] K. Watari, T. Nagaoka, S. Kanzaki, Densification process of α′ sialon ceramics, J. Mater. Sc. 29 (22) (1994) 5801–5807.
[16] J.W. Min, M. Mitomo, Preparation of Y-α-sialon with glassy or crystalline phases at grain boundaries, Ceram. Intern. 21 (6) (1995) 427–32.
[17] A. Ashkin, D. Ashkin, O. Babushkin, T. Ekstrom, At- Temperature observation of phase development in yttrium α-sialon, J. Eur. Ceram. Soc. 15 (11) (1995) 1101–1109.
[18] S. Bandyopadhyay, M.J. Hoffmann, G. Petzow, Densification behaviour and properties of Y_2O_3-containing α-sialon based composites, J. Am. Ceram. Soc. 79 (6) (1996) 1537–1545.
[19] S. Hampshire, K.P.J. O'Reilly, L. Leigh, M. Redington, Formation of α′-sialon with neodymium and samarium modifying cations, in: P. Vincenzini (Ed.), High Tech Ceramics, Elsevier Science Publishers B. V., Amsterdam, Netherlands, 1983, 933–940.
[20] P.O. Kall, T. Ekstrom, Sialon ceramics made with mixtures of Y_2O_3-Nd_2O_3 as sintering aids, J. Eur. Ceram. Soc. 6 (2) (1990) 119–127.
[21] T. Ekstrom, K. Jansson, P.O. Olsson, J. Persson, Formation of an Y/Ce doped α-sialon phase, J. Eur. Ceram. Soc. 8 (1) (1991) 3–9.
[22] M. Redington, S. Hampshire, Multication α-sialon, Brit. Ceram. Proc. 49 (1992) 175–190.

[23] P.L. Wang, W.Y. Sun, T.S. Yen, Formation and densification of R- α′-SiAlONs (R = Nd, Sm, Gd, Dy, Er, Yb), in: I.W. Chen, P.F. Becher, M. Mitomo, G. Petzow, T.S. Yen (Eds.), Silicon Nitride Ceramics-Scientific and Technological Advances, Mater. Res. Soc., Pittsburg, USA, 1993, 287, 387–392.
[24] K.P.J. O'Reilly, M. Redington, S. Hampshire, M. Leigh, Parameters affecting pressureless sintering of α′-sialons with lanthanide modyfying cations, ibid, 1993, 393–398.
[25] Y.B. Cheng, D.P. Thompson, Preparation and grain boundary devitrification of samarium α-sialon ceramics, J. Eur. Ceram. Soc. 14 (1994) 13–21.
[26] Y.B. Cheng, D.P. Thompson, Pressureless sintering and phase relationship of samarium α sialon, J. Eur. Ceram. Soc. 14 (4) (1994) 343–349.
[27] P.L. Wang, W.Y. Sun, T.S. Yen, Sintering and formation behaviour of R-α-sialon (R = Nd, Sm, Gd, Dy, Er, Yb), Eur. J. Solid State Inorg. Chem. 31 (93) 104.
[28] H. Mandal, N. Camuscu, D.P. Thompson, Comparisons of the effectiveness of rare earth sintering additives on the high temperature stability of α-sialon ceramics, J. Mater. Sc. 30 (23) (1995) 5901–5909.
[29] Z. Shen, T. Ekstrom, M. Nygren, Temperature stability of samarium doped α-sialon ceramics, J. Eur. Ceram. Soc. 16 (1) (1996) 43–53.
[30] Z. Shen, T. Ekstrom, M. Nygren, Homogeneity region and thermal stability of neodymium- doped α- sialon ceramics, J. Am. Ceram. Soc. 79 (3) (1996) 721–732.
[31] Y.B. Cheng, D.P. Thompson, Aluminium containing nitrogen melilite phases, J. Am. Ceram. Soc. 77 (1) (1994) 143–148.
[32] Z.-K. Huang, I.-W. Chen, Rare earth melilite solid solution and its phase relations with neighboring phases, J. Am. Ceram. Soc. 79 (8) (1996) 2091–2097.
[33] S.L. Hwang, I.-W. Chen, Reaction hot pressing of α′- and β′- SiAlON ceramics, J. Am. Ceram. Soc. 77 (1) (1994) 165–171.
[34] A. Nagel, P. Greil, G. Petzow, Reaction sintering of yttrium containing α-silicon nitride solid solution, Revue de Chimie Minerale t22 (1985) 437–448.
[35] G.R. Antis, P. Chantikul, B.R. Lawn, D.B. Marshal, A critical evaluation of indentation techniques for measuring fracture toughness, J. Am. Ceram. Soc. 64 (9) (1981) 533–338.
[36] H. Mandal, D.P. Thompson, T. Ekstrom, Reversible α↔β sialon transformation in heat treated sialon ceramics, J. Eur. Ceram. Soc. 12 (1993) 421–429.
[37] R. Zhao, Y.-B. Cheng, Phase transformation in Sm (α + β)- SiAlON ceramics during post-sintering heat treatments, J. Eur. Ceram. Soc. 15 (12) (1995) 1221–1228.
[38] W.Y. Sun, P.L. Wang, D.S. Yan, Phase transformation in Ln-(α + β)-sialon ceramics by heat treatment, Mater. Lett. 26 (1–2) (1996) 9–16.
[39] R. Zhao, Y.B. Cheng, J. Drennan, Microstructural features of the α to β- SiAlON phase transformation, J. Eur. Ceram. Soc. 16 (5) (1996) 529–534.
[40] Z. Shen, T. Ekstrom, M. Nygren, Reactions occurring in post heat treated α/β sialons : On the thermal stability of α- sialon, J. Eur. Ceram. Soc. 16 (8) (1996) 873–883.
[41] S. Bandyopadhyay, The in-situ formation of sialon composite phases, J. Eur. Ceram. Soc. 17 (7) (1997) 929–934.